International Symposium on
HYDROACOUSTICS AND ULTRASONICS
EAA Symposium (formerly 13th FASE Symposium)
Gdańsk-Jurata, 12-16 May 1997

Scattering of Focused Strong Pressure Pulses by Spheroids

E. Steiger
Institut für Höchstfrequenztechnik und Elektronik / Akustik, Universität Karlsruhe
Kaiserstraße 12, D-76128 Karlsruhe, Germany

ABSTRACT

A two-dimensional finite-difference in time-domain (FDTD) discretization is applied to simulate finite amplitude sound pulse propagation in a reflector-focusing lithotripter. The FDTD-model is verified by the comparison of wave profiles predicted by the model with measured ones in the focal region. Special interest is set on a correct and stable modeling of spheroids with rigid or pressure release surfaces representing different scatterers modifying the pulsed pressure field in the applications. The resulting curved boundaries to be represented on a Cartesian grid tend to generate short spurious numerical waves which may lead to numerical instability. A method is presented to include arbitrarily curved boundaries in a stable manner into the underlying rectangular grid. It is verified by the comparison of the analytical solution of a simple one-dimensional scattering problem with corresponding numerical results. Using the curved boundary technique different spheroidal scatterers are included into the lithotripter model. Their influences on the significant field parameters are demonstrated. Even the conditions on the surfaces which may be of interest for simulating the interactions of kidney stones or gaseous bubbles with incident pulses of the spheroids are computable.

INTRODUCTION

Focused strong pressure pulses and shock waves are used in different biomedical applications like in lithotripsy. The therapeutical efficiency depends on field parameters like the amplitudes of the pressure pulse or the contributions of its energy to positive pressure, negative pressure and shocked components. Beneath the influence of absorbing effects in layers of human tissue therefore the modifications of the sound pulse due to scattering on body stones, gaseous cavities or negative pressure induced cavitation bubbles are of interest. Their investigation requires a flexible numerical tool with only a moderate need for computational cost. That is why the method of choice is based on an finite-difference time-domain (FDTD) discretization of a set of equations approximating the Navier-Stokes equations [1]. As nonlinear pulse and weak shock propagation is considered the FDTD-model must represent the propagation of waves of even short rise times correctly whereas spurious short wave components are dropped. To realize this economically a dispersion relation preserving (DRP) algorithm [2] is applied on the system of nonlinear equations.

The studies presented in this paper are carried out using a model of the Storz lithotripter SL 10 [3]. This model is verified by comparison of computed and measured wave profiles in the focal region. The interaction of the corresponding pulse with the scatterers represented by spheroids is investigated.

MATHEMATICAL MODEL

A mathematical model is realized with a system of partial differential equations. Usually shocked solutions are excluded in acoustic approaches. Fortunately shock waves occuring in biomedical applications are shocks of weak character in the sense of fluid dynamics. They may be represented in a numerical scheme using approximations of second order in nonlinearity of the Euler equations. Thus it is possible to limit the originally big scales of the relevant quantities dealing only with their (acoustic) perturbations [1]:

$$\frac{\partial \rho}{\partial t} + \rho_0 \nabla \cdot \vec{u} = -\nabla \cdot (\rho \vec{u}) \qquad (1a)$$

$$\rho_0 \frac{\partial \vec{u}}{\partial t} + \nabla p = \frac{\rho}{\rho_0} \nabla p - \rho_0 \vec{u} \cdot \nabla \vec{u} \qquad (1b)$$

(1a) and (1b) are approximations of the equations of continuity and momentum, respectively.

To close the system of equations a nonlinear equation of state is applied also valid up to the second order of nonlinearity:

$$p = c_0^2 \rho + \frac{c_0^2}{\rho_0} \frac{B}{2A} \rho^2 \qquad (2)$$

ρ is the acoustic perturbation of the fluids mass density ρ_0 at atmospheric pressure p_0. $\vec{u}$ is the velocity vector and p the acoustic pressure. c_0 represents sound velocity, $B/2A$ the acoustic parameter of nonlinearity. Effects of (weak) dissipation and dispersion even relaxation may be represented by additional equations.

As indicated above with the conditions $|\vec{u}|_{max} << c_0$ or $p_{max}/E << 1$ (with E being the fluid's bulk modulus; $E_{water} \approx 2.2$GPa) equations (1) and (2) may include the (nonlinear) shock effects adequately. In the applications the maximum pressures are of the order of 100MPa [4].

A correct shock representation in velocity and amplitude (and anomalous dissipation) in the limit of vanishing mesh sizes requires the fulfillment of the conditions of the Lax-Wendroff theorem. Therefore (1) has to be formulated in conservation form [5]:

$$\frac{\partial \vec{w}}{\partial t} + \begin{pmatrix} \dfrac{\partial F_1(\vec{w})}{\partial x_1} \\ \vdots \\ \dfrac{\partial F_{N+1}(\vec{w})}{\partial x_{N+1}} \end{pmatrix} = \begin{pmatrix} S_1\left(\vec{w}, \dfrac{\partial \vec{w}}{\partial x_1}, .., \dfrac{\partial \vec{w}}{\partial x_N}\right) \\ \vdots \\ S_{N+1}\left(\vec{w}, \dfrac{\partial \vec{w}}{\partial x_1}, .., \dfrac{\partial \vec{w}}{\partial x_N}\right) \end{pmatrix} \qquad (3)$$

with

$$\vec{w} = \left(\rho,\ u_1,\ \cdots,\ u_N\right)^T \qquad (4)$$

and $F_i(\vec{w})$ being arbitrary nonlinear functions of $\vec{w}$. For a two-dimensional ($N = 2$) axisymmetrical geometry as presumed here x_1 and x_2 turn out to be r and z, respectively.

NUMERICAL MODEL

On the one hand the expected solutions have a smooth character over wide parts of the computational domain. On the other especially the short components representing shocks are of particular interest. In order to include these huge time scales as economically as possible, a FDTD-scheme has to be designed with a large "bandwidth" related to the available number of points-per-wavelength (ppw). In this presentation a DRP-algorithm [2] is taken as a basis for the discretization of (1) in the form of equation (3). The algorithm has to be formulated as a conservative method in the sense of Lax and Wendroff [5]. Additional relations that must be fulfilled by the field parameters as equations of state (2) or dispersion-dissipation relations are fully integrable into the DRP-algorithm or parallely solved after every time step. This does not require much additional computational costs.

A second-order artificial viscosity is applied to eliminate spurious oscillations. Following [2] a wave-number dependent dimensionless damping function $\tilde{D}(k\Delta x)$ is designed with a low-pass filter character. k and Δx are the wave-number of the signal and the computational grid's mesh size, respectively.

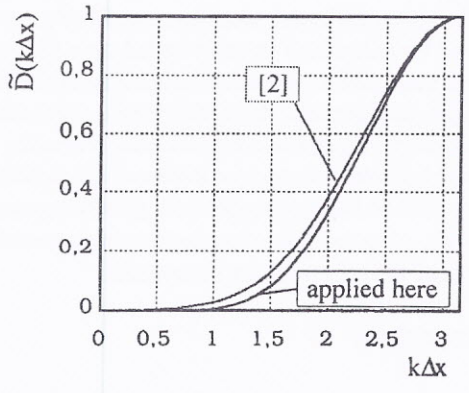

Fig.1 Fourier transform $\tilde{D}(k\Delta x)$ of the artificial selective damping terms

Fig. 1 shows $\tilde{D}(k\Delta x)$ from "∞" ppw ($k\Delta x = 0$) to 2 ppw ($k\Delta x = \pi$). The function moves smoothly from "no damping" ($\tilde{D} = 0$) of long waves to "maximum damping" ($\tilde{D} = 1$) of waves being represented by only two grid points. The proposal given in [2] has been modified to get a better filter-character for the mentioned applications.

In combination with the scheme's inherent numerical viscosity the artificial selective damping is modeling the anomalous dissipation of energy in the shock front with second-order accuracy. This holds provided that a flux representation (3) is taken as a basis.

A verification especially of the modeled losses due to shock propagation is performed by a comparison with Blackstock's one-dimensional results for cylindrically diverging sinusoidal waves of finite amplitude [6]. A 100kHz sine wave is radiated from an infinite

cylinder with a radius of 4cm into a fluid with the acoustic properties of water at 20°C (c_0 = 1481ms^{-1}, B/A = 5). At the cylinder's surface the radial component of the velocity is 21.4ms^{-1} (corresponding to a shock distance of 10cm). The "recorded" wave profiles of the analytical, the numerical results and the solution with assumed linear propagation are compared at a radius of 20cm (fig. 2).

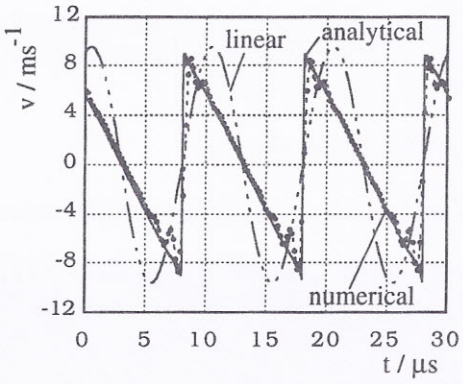

Fig.2 Linear (dashed) and finite amplitude (analytical: continous, numerical: with dots) continous wave solutions for a cylindrically diverging wave at r = 20cm

For the high intensities assumed the comparison with the linear result shows a strong anomalous dissipation in the analytical as well as in the numerical solution. The excellent agreements of the zeros even in the shock locations demonstrate a correct reproduction of the phase velocities even of the short wave components. This is enabled by the DRP-algorithm fulfilling the Lax-Wendroff theorem.

To limit the computational domain absorbing boundaries have to be implemented. The basic equations are transformed locally in the boundary regions into the characteristic form in order to decouple the boundary treatment from time integration. So the waves are separated into components entering and leaving the computational domain. Combined with a little amount of artificial viscosity the applied method results in good absorber qualities [7].

CURVED BOUNDARIES

When multi-dimensional problems are considered a regular Cartesian grid is generally preferable for acoustic wave propagation problems. Therefore the modeling of arbitrary curved surfaces requires a method taking into account that the corresponding curved boundaries intersect lines of the grid at points being no mesh points generally (fig. 3). To keep the high-order character of the scheme and to enable an accurate modeling of an object's curved surface in [8] a boundary treatment based on the application of asymmetric difference stencils is proposed. Implicitly the boundary conditions are fulfilled approximately on the intersection points by interpolation. Using artificial selective damping this method works quite well for (inner) boundary lengths of not too many Δx. For bigger objects it fails. The asymmetric stencils generate too strong spurious short wave components that finally lead to instability.

Therefore the exclusive use of central symmetric difference stencils to approximate the spatial derivatives even in closest proximity to the curved boundaries is proposed. This requires the determination of values in so called ghost points G outside the inner ("fluidal") domain (the fluidal domain further is called inner region) to keep approximately the conditions on the curved boundary (fig. 3). Those ghost values have to be computed using information from within the inner region, more precise from inner region points (source points S) each attached to one ghost point. The line GS intersects the curved boundary rectangularly in its midpoint (fig. 3). The generally time and space dependent operator $T: \vec{w}|_S \rightarrow \vec{w}|_G$ providing the ghost value is supplied by the character of the (local) boundary condition. Since the source points mostly are no grid points the source values have to be interpolated and extrapolated, respectively.

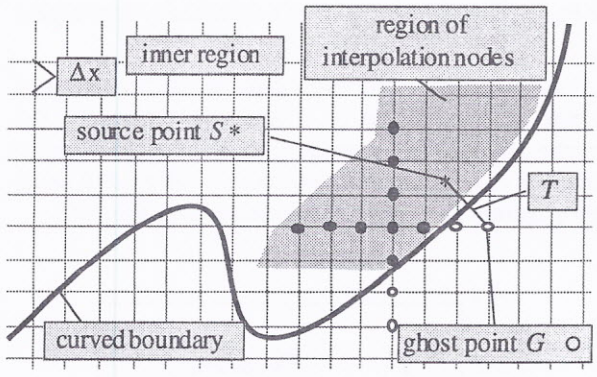

Fig.3 Modeling a curved boundary in the Cartesian grid

The interpolation method applied has to fulfill two main conditions. On the one hand it must be of higher order to keep accuracy in the boundary region on the other only a minimum amount of spurious short wave components are allowed to be generated to keep stability. Therefore bicubic splines [9] are applied. With a medium number of interpolation nodes (in the presented simulations around 25 were used) they properly fulfill the requirements mentioned. In determining the set of interpolation nodes (fig. 3) which belong to one source point attention must be paid. The sets sup-

plying two neighboring source points must be the more similar the shorter the distance is inbetween. The numerical algorithm for the attachment of the interpolation nodes to the source points is performed only once namely in the preprocessing part of the computer run.

Compared to the method proposed in [8] beneath a much bigger robustness higher accuracy is obtained as every *S-G* pair stands for one tangent approximating the curved boundary (fig. 3). The price are additional computational costs which are small compared to the total ones although the procedure has to be performed before every time step.

To verify the presented method a simple "1D scattering problem" is considered.

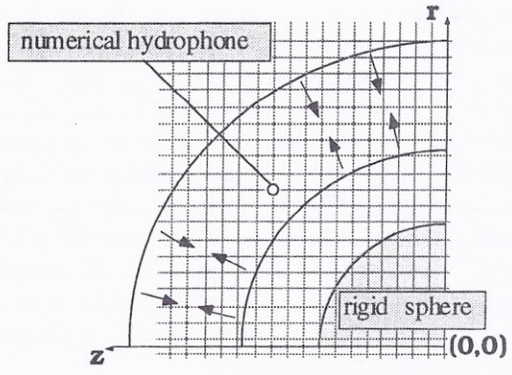

Fig.4 Numerical model of a spherically converging pulse interacting with a rigid sphere

A spherically converging pulse of the length of about 23 Δx impinges on a rigid sphere placed in the center (fig. 4). The wave profile of the incident pulse is taken to be a damped sinusoidal function. For linear propagation an analytical solution is available [10].

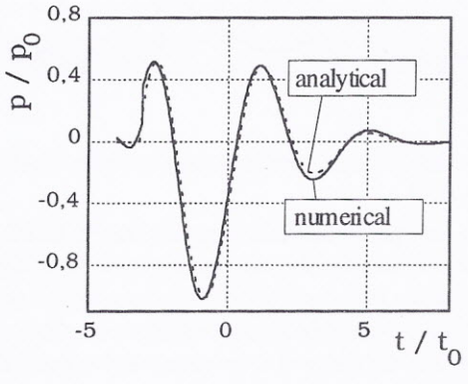

Fig.5 Analytically and numerically obtained wave profiles of the reflected diverging pulse

The numerical solution is obtained solving (1) and (2) reduced to linear propagation in cylindrical coordinates with *r*- and *z*- dependency (fig. 4). The boundary conditions on the sphere's surface (the radius of curvature is seven Δx) are fulfilled applying the method proposed. The comparison of a wave profile recorded by a "numerical hydrophone" (fig. 4) with the analytical result shows very good agreements independent of the pulse's propagation direction relative to the grid (fig. 5). They are obtained even in the case of the radius of the sphere being two Δx only. For numerical stability a weak artificial viscosity (see above) is sufficient. The limiting factor remains to be dictated by the minimum resolution of the wave for propagation computation.

MODEL OF THE SL 10

The Storz SL 10 is a reflector-focused lithotripter [3].

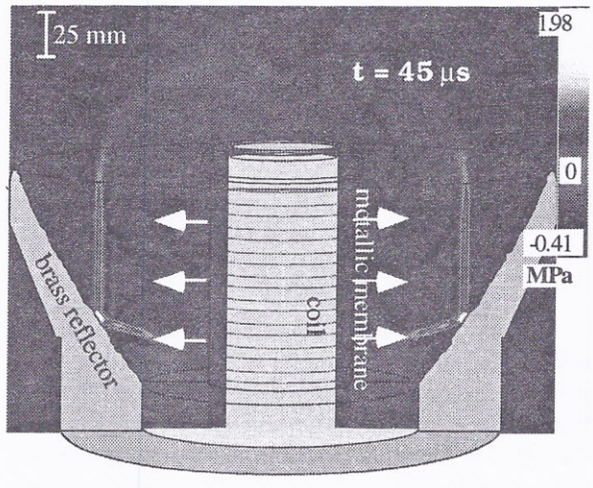

Fig.6 Pressure profile 45µs after onset of pulse generation

The sound pulse is radiated from a cylindrical electromagnetic transmitter (fig. 6). A discharge process conducted through a cylindrical coil induces eddy currents on a metallic membrane. The enforced move in radial direction has a duration in the order of microseconds and generates the diverging cylindrical wave front.

The process beginning with sound pulse radiation continuing with reflection at the solid brass reflector and ending after passing the focal region is computed and visualized in figs. 6 and 7. The simulated reflection at the paraboidal brass works in a stable manner. The maximum pressure on the metallic membrane is assumed to be 1.65MPa.

The excellent agreements of measured (the measurements were performed using a PVDF needle-hydrophone) and predicted wave profiles in positions out of the focus demonstrate the accurate modeling of the curved (!) reflector again (fig. 8).

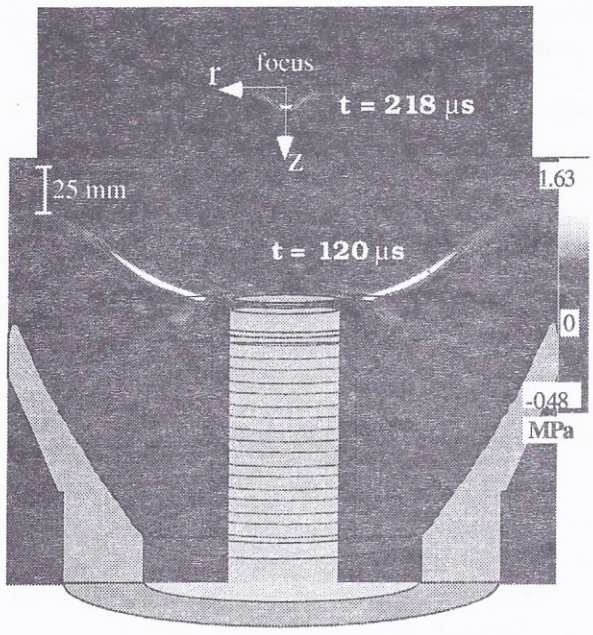

Fig.7 Pressure profiles 120µs and 218µs after onset of pulse generation

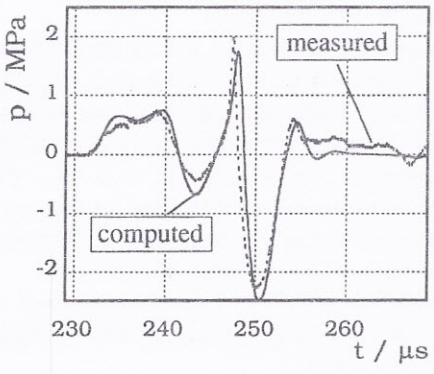

Fig.8 Measured and predicted wave profiles in position (z = -30mm, r = 20mm)

The comparison in the focus (z = 0, r = 0) shows deviations in the negative pressure parts and in the shock's absolute amplitude (fig. 9). Here an underestimation of the computed shock's height meets an overestimation of the measured result obtained with a probe of finite size. Further PVDF needle-hydrophones are known to underestimate stronger transient negative pressures. Therefore the computed wave profile seems to be more realistic since there are deviations only in the closest focal region.

The excellent agreements of the zeroes and the amplitudes demonstrate the suitability of the method for the named applications as a whole.

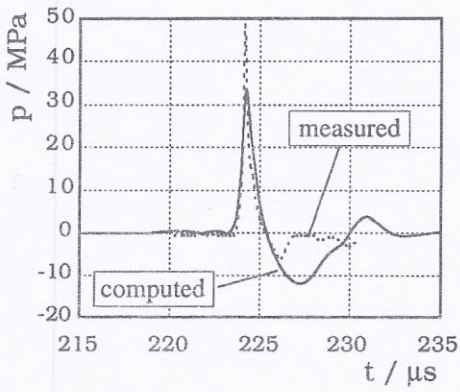

Fig.9 Measured and predicted wave profiles in the focus (z = 0, r = 0)

SCATTERING AT A RIGID ELLIPSOID IN THE FOCAL REGION

The pulse predicted by the numerical model is taken as initial data to compute the scattering process with a rigid ellipse of length 1cm and width 3mm. The ellipse is placed in the focus with one of its tips (figs. 10 to 12). After 223µs (from onset of pulse generation on the radiating cylinder) the main pulse incidents on the scatterer (fig. 10). Later a spherically diverging scattering wave consisting of shorter wave components is generated with the tip of the ellipse as its center (among others these are supposed to consist of the shocked components in reality). The longer components are interacting only weakly with the scatterer (figs. 11 and 12).

Even in this severe "test run" the numerical simulation remains stable. Further field parameters on the scatterer's surface are determinable easily.

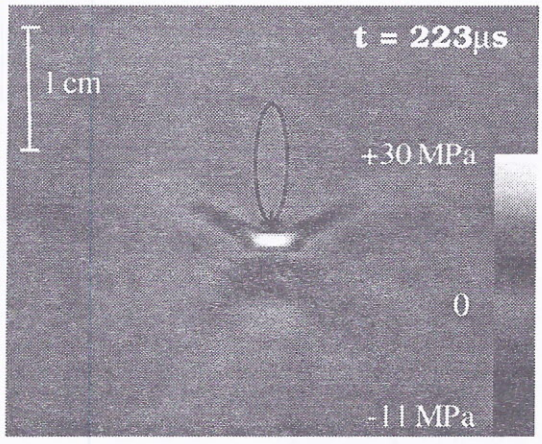

Fig.10 Reflector focused shocked pulse incident on a rigid ellipse

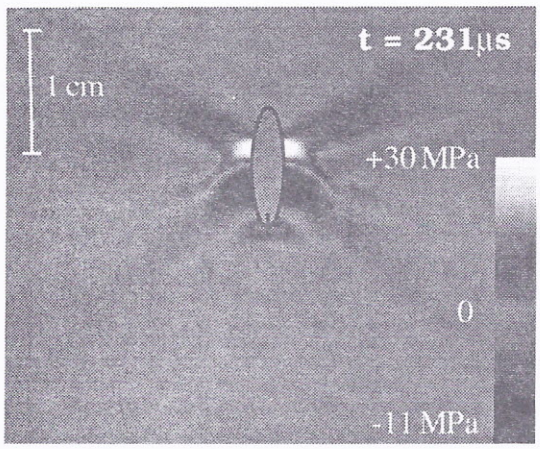

Fig.11 Same process 8µs later

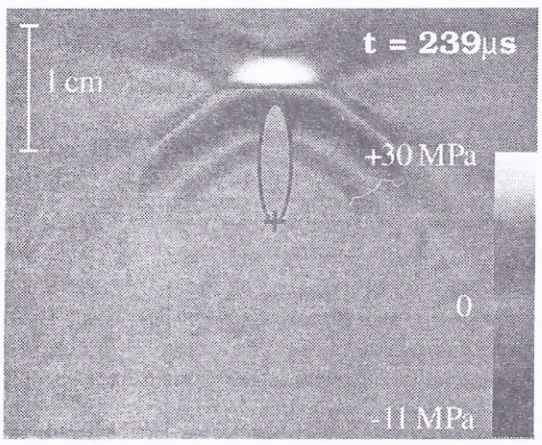

Fig.12 The pulse has passed the ellipse. Shorter components have been scattered at the tip in the focus (+).

CONCLUSIONS

The curved boundary treatment proposed remains accurate and stable even when large surfaces are modeled. In combination with a specific DRP-algorithm it turns out to be a flexible tool for computing the propagation of biomedically applied high pressure pulses under presence of scatterers or generally curved (inner) boundaries. On the curved surfaces pressure- and velocity-time histories are computable by the proposed method in high-order accuracy like in inner-region points. Shock waves being reproduced correctly in amplitude and anomalous dissipation incident on curved boundaries remain numerically stable too.

ACKNOWLEDGMENTS

This work was supported by the Deutsche Forschungsgemeinschaft (Gz.: Wi 1044/3) and by Storz Medical, Tuttlingen, Germany. The measurements in the field of the SL10 were carried out by Storz.

REFERENCES

1. Sparrow, V. W., (1993), Time Domain Computations in Nonlinear Acoustics Without One-Way Assumptions, J. Comp. Acoust., **1**, 359-369
2. Tam, C.K.W., Webb, J.C., Dong, Z. (1993), A Study of the Short Wave Components in Computational Acoustics, J. Comp. Acoust., **1**, 1-30
3. Wess, O., Marlinghaus, E.H., Katona, J., (1989), Eine großaperturige Leistungsschallquelle für medizinische Anwendungen, DAGA '89 Proceedings, Duisburg, 295-298
4. Delius, M., (1994), Medical Applications and Bioeffects of Extracorporal Shock Waves, Shock Waves, **4**, 55-72
5. LeVeque, R., (1992), Numerical Methods for Conservation Laws, Birkhäuser, Basel, Boston, Berlin
6. Blackstock, D.T., (1966), Connection between the Fay and Fubini Solutions for Plane Sound Waves of Finite Amplitude, J. Acoust. Soc. Am, **39**, 1019-1026
7. Steiger, E., Riedlinger, R.E., (1995), Numerical and Experimental Investigation of Strongly Focused High Pressure Pulses, Ultrasonics World Congress Proceedings, Berlin, 163-166
8. Kurbatskii, K.A., Tam, C.K.W., (1997), Cartesian Boundary Treatment of Curved Walls for High-Order Computational Aeroacoustic Schemes, AIAA Journal, **35**, 133-140
9. Späth, H., (1995), Two Dimensional Spline Interpolation Algorithms, AK Peters, Wellesley, Massachusetts
10. Landau, L.D., Lifshitz, E.M., (1987), Fluid Mechanics, Pergamon Press, Oxford